doi:10.1016/j.ymthe.2004.08.027

ARTICLE

Liver-directed Neonatal Gene Therapy Prevents Cardiac, Bone, Ear, and Eye Disease in Mucopolysaccharidosis I Mice

Yuli Liu,[1] Lingfei Xu,[1] Anne K. Hennig,[1] Attila Kovacs,[1] Annabel Fu,[1] Sarah Chung,[1] David Lee,[1] Bin Wang,[1] and Ramin S. Herati[1] Judith Mosinger Ogilvie[2] Shi-Rong Cai[1] Katherine Parker Ponder[1,3,*]

[1]*Department of Internal Medicine,* [2]*Department of Ophthalmology and Visual Sciences, and* [3]*Department of Biochemistry and Molecular Biophysics, Washington University School of Medicine, St. Louis, MO 63110, USA*

**To whom correspondence and reprint requests should be addressed at the Department of Internal Medicine, Washington University School of Medicine, 660 South Euclid Avenue, St. Louis, MO 63110. Fax: +1 314 362 8813. E-mail: kponder@im.wustl.edu.*

Mucopolysaccharidosis I (MPS I) due to deficient α-L-iduronidase (IDUA) activity results in accumulation of glycosaminoglycans in many cells. Gene therapy could program liver to secrete enzyme with mannose 6-phosphate (M6P), and enzyme in blood could be taken up by other cells via the M6P receptor. Newborn MPS I mice were injected with 10^9 (high dose) or 10^8 (low dose) transducing units/kg of a retroviral vector (RV) expressing canine IDUA. Most animals achieved stable expression of IDUA in serum at 1240 ± 147 and 110 ± 31 units/ml, respectively. At 8 months, untreated MPS I mice had aortic insufficiency, increased bone mineral density (BMD), and reduced responses to sound and light. In contrast, MPS I mice that received high-dose RV had normal echocardiograms, BMD, auditory-evoked brain-stem responses, and electroretinograms. This is the first report of complete correction of these clinical manifestations in any model of mucopolysaccharidosis. Biochemical and pathologic evaluation confirmed that storage was reduced in these organs. Mice that received low-dose RV and achieved 30 units/ml of serum IDUA activity had no or only partial improvement. We conclude that high-dose neonatal gene therapy with an RV reduces some major clinical manifestations of MPS I in mice, but low dose is less effective.

Key Words: gene therapy, lysosomal storage disease, retroviral vector, mucopolysaccharidosis, glycosaminoglycan, neonatal, liver, mannose 6-phosphate

INTRODUCTION

Lysosomal storage diseases (LSD) have an overall incidence of ~1:7700 live births [1] and are caused by deficient activity in lysosomal enzymes that degrade various molecules. LSD are currently treated with bone marrow transplantation (BMT) or enzyme replacement therapy (ERT). ERT usually involves intravenous (iv) administration of enzyme containing mannose 6-phosphate (M6P), which is taken up by cells throughout the body via the M6P receptor (M6PR) [2]. One exception is the enzyme used for ERT for Gaucher disease, which contains oligosaccharides with terminal mannose residues and is taken up by cells of the reticuloendothelial system via the mannose receptor.

An alternative approach to treating LSD is to use liver-directed gene therapy to program hepatocytes to secrete enzyme with M6P into blood. Retroviral vectors (RV), adenovirus-associated virus (AAV) vectors, and adenoviral vectors have all transduced liver cells and exerted a beneficial effect in LSD (reviewed in [3]). The mucopolysaccharidoses (MPS) involve the inability to degrade glycosaminoglycans (GAGs) [4]. Neonatal RV-mediated gene therapy has successfully treated both mice and dogs with MPS VII [5–7], which is due to deficient β-glucuronidase (GUSB) activity. Intravenous injection of RV within 3 days after birth resulted in stable transduction of 20 and 2% of hepatocytes in mice [5] and dogs [8], respectively. In mice, the liver was clearly the major site of both transduction and expression when an RV with the human α_1-antitrypsin promoter was used, as RV DNA and RNA levels were >10- and >100-fold higher, respectively, in liver than in other organs at 6 months after transduction [5]. Enzyme with M6P was secreted into blood, and enzyme activity was high in organs with little or no RV RNA, suggesting that cells had taken up GUSB from

1525-0016/$30.00

doi:10.1016/j.ymthe.2004.08.027

blood via the M6PR. However, BM cells were also stably transduced after iv injection of RV into newborns. Furthermore, they expressed GUSB from the long terminal repeat (LTR) of the RV at 6 weeks after birth, although expression was very low at late times [7,9], presumably due to inactivation of the LTR. Thus, both uptake of enzyme from blood and short-term expression in BM-derived cells might contribute to the therapeutic effect of this neonatal RV-mediated gene therapy approach.

Although gene therapy has been beneficial in animals with MPS VII, cartilage and bone disease were not completely corrected with administration of any vector [10]. Furthermore, only partial improvements were observed in hearing after AAV vector-mediated gene therapy [11] or in visual function after BMT [12] or localized AAV vector-mediated gene therapy [13] and have not been evaluated after systemic administration of the other vectors. Cardiac function was almost completely corrected in dogs after neonatal RV-mediated gene therapy [14], but has not been evaluated in mice. Thus, many of the major clinical manifestations of disease in MPS VII, the most widely studied model, have not been prevented to date. It is possible that the large size of the tetrameric GUSB protein (~340 kDa) as well as the relatively high enzyme levels present in most organs will make it difficult to achieve sufficient levels to correct the disease completely. An additional problem with MPS VII is that it is very rare in humans, and it may be difficult to identify sufficient numbers of patients to test the efficacy of this approach.

MPS I is an autosomal recessive disorder due to deficiency of α-L-iduronidase (IDUA; EC 3.2.1.76) that results in the accumulation of heparan and dermatan sulfate [4]. Patients with severe disease (Hurler syndrome; OMIM 607014) have cardiac disease, skeletal deformities, hearing and visual abnormalities, and mental retardation. Patients with intermediate disease (OMIM 607015) have similar somatic manifestations without neurological disease. Patients with mild disease (Scheie syndrome; OMIM 607016) have somatic manifestations of reduced severity. MPS I has an incidence of 1:100,000 live births [15] and is much more common than MPS VII. This should make it possible to identify patients to treat should any gene therapy approach prove to be efficacious and safe. The existence of mouse [16,17], cat [18], and dog [19,20] models of MPS I will facilitate preclinical testing of novel therapeutic approaches. Furthermore, IDUA is relatively small (~70 kDa) [4] and the normal IDUA activity is low, which might make it easier to obtain correction for MPS I than for MPS VII. Finally, achieving only 5% of normal activity in the appropriate cells may prevent disease manifestations, as the enzyme activity in fibroblasts from Scheie patients is below this value [21,22]. Others have previously reported that RV-mediated BM-directed [23] or neonatal AAV vector-mediated [24] gene therapy can reduce some aspects of disease in MPS I, but many of the clinical manifestations have not yet been evaluated. We therefore tested the effects of neonatal liver-directed RV-mediated gene therapy in mice with MPS I

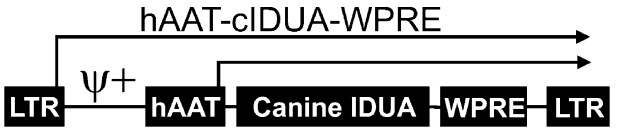

FIG. 1. Retroviral vector hAAT-cIDUA-WPRE. The Moloney murine leukemia virus-based RV contains intact long terminal repeats (LTR) at the 5′ and 3′ ends, an extended packaging signal (ψ^+), the human α_1-antitrypsin promoter (hAAT), the canine α-L-iduronidase (IDUA) cDNA, and the woodchuck hepatitis virus posttranscriptional regulatory element (WPRE). Transcription can initiate from the LTR or the hAAT promoters as indicated by the arrows.

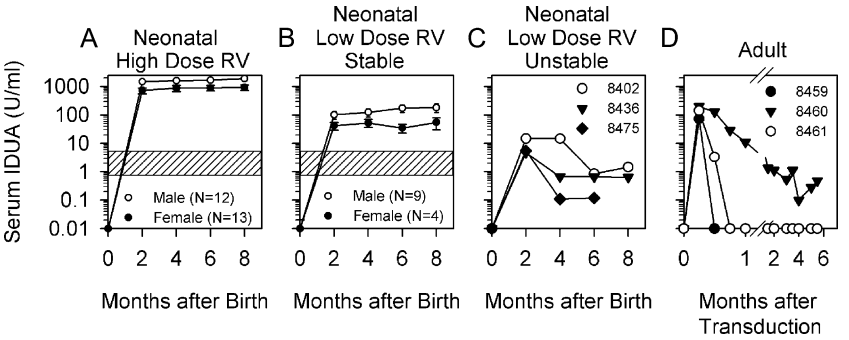

FIG. 2. Serum IDUA activity. (A) High-dose RV to newborns. MPS I mice received 10^9 TU/kg hAAT-cIDUA-WPRE at 2–3 days after birth, and the serum IDUA was determined at the indicated time after birth. Average values for males and females ± SEM are shown. The values of <0.01 U/ml at 0 months represent levels present in adult untreated MPS I mice. The average values in homozygous normal mice of 2.2 ± 1.6 U/ml (±2 standard deviations) are indicated by the shaded area. (B) Low-dose RV to newborns that maintained expression. MPS I mice received 10^8 TU/kg hAAT-cIDUA-WPRE at 2–3 days after birth, and average levels of IDUA ± SEM are shown for mice that maintained stable expression. (C) Low-dose RV to newborns that lost expression over time. MPS I mice were treated with low-dose RV as described for B, but lost expression of IDUA in serum over time. Serum IDUA activity for individual mice is shown. (D) RV to adult mice. Adult mice were injected with 1.9×10^9 TU/kg after administration of HGF to induce replication of hepatocytes. Serum IDUA activity for individual mice is shown.

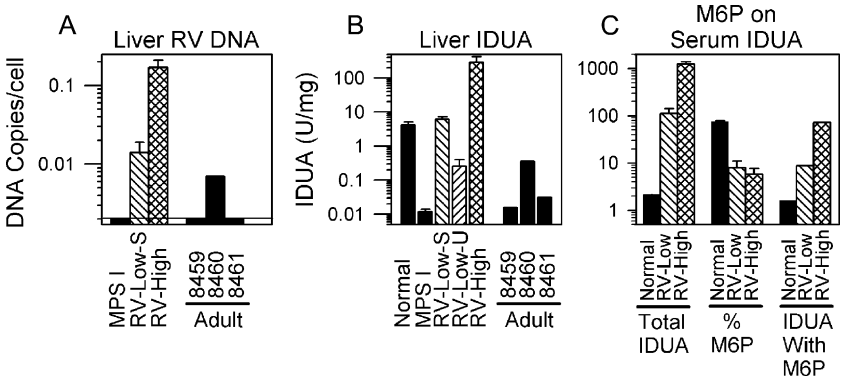

FIG. 3. Liver RV DNA and IDUA activity, and M6P content of serum IDUA. Animals were treated as described for Fig. 2, and samples were obtained at 8 months for most animals. Liver biopsy samples were obtained at 2 months after gene therapy for mice treated as adults. (A) RV DNA copy number. The RV DNA copy number in the liver per diploid genome ± SEM was determined for animals that received low-dose (RV-Low-S; $N = 5$) or high-dose (RV-High; $N = 5$) RV and maintained expression over time. Two nontransduced MPS I mice had no detectable RV DNA sequences (<0.002 copies per cell), which is shown as a line at the bottom. Individual values are shown for mice that received gene transfer as adults. (B) IDUA activity. Liver IDUA activity was determined for homozygous normal ($N = 4$) and MPS I ($N = 4$) mice, for animals with stable expression that received neonatal injection of low-dose RV ($N = 4$) or high-dose RV ($N = 4$), for animals that received low-dose RV as newborns and had unstable expression (RV-Low-U; $N = 2$), or for animals that received RV as adults and had unstable expression (Adult; values for individual animals are shown). (C) Percentage serum IDUA with M6P. The left bars show the average serum IDUA activity in U/ml ± SEM for normal or RV-treated mice with stable expression. The middle bars show the percentage of serum IDUA activity that was retained on a M6PR column using samples obtained at 4 to 8 months after birth. The right bars show the calculated amount of IDUA activity with M6P in serum in U/ml.

upon cardiac function, bone, hearing, and vision. We demonstrate here that this approach completely corrects these manifestations.

RESULTS

Generation of an RV Expressing Canine cIDUA

We cloned the canine IDUA cDNA into an RV to generate hAAT-cIDUA-WPRE (Fig. 1) and used a high-titer amphotropic clone to prepare the RV. We chose the canine IDUA as this study in mice will be followed by experiments in dogs, and we wanted to use the canine gene for the dog study. We transduced mouse fibroblast 3521 cells with dilutions of RV and prepared DNA and protein extracts 1 week later. The DNA copy number determined by real-time PCR demonstrated that the average titer was ~2×10^7 transducing units (TU)/ml. IDUA enzyme activity in cell extracts was 1152 ± 121 [standard error of the mean (SEM)] U/mg after normalization to 1 copy of RV per diploid cell. This activity was >500-fold higher than in nontransduced 3521 cells.

Serum Activity After *in Vivo* Transduction of MPS I Mice

MPS I mice that were injected shortly after birth with 10^9 or 10^8 TU/kg hAAT-cIDUA-WPRE will be referred to hereafter as being treated with high-dose or low-dose RV, respectively. Untreated MPS I mice will be referred to hereafter as MPS I mice. All high-dose RV mice expressed IDUA in serum at stable levels for 8 months. Levels in males (1659 ± 170 U/ml) were approximately twofold higher than in females (854 ± 180 U/ml; $P = 0.003$ using Student's t test), as shown in Fig. 2A. For the low-dose RV mice, 13 of 17 expressed IDUA at stable levels for 8 months, as shown in Fig. 2B. Expression was higher in males (146 ± 44 U/ml) than in females (47 ± 13 U/ml), although these were not statistically different. Of the remaining mice, 3 that had >5 U/ml of serum IDUA activity at 2 months lost activity over time (Fig. 2C), while 1 had very low levels at all times (data not shown). Three adult mice were injected with 2×10^9 TU/kg RV after hepatocyte replication was induced with hepatocyte growth factor (HGF). These mice achieved 138 ± 36 U/ml IDUA activity in serum at 1 week, but activity fell thereafter to undetectable levels in 2 animals and low levels (~1 U/ml) in 1 animal (Fig. 2D).

DNA Copy Number in Liver

The DNA copy number at 8 months after birth in animals that maintained expression at stable levels after neonatal transfer was 0.014 ± 0.005 and 0.17 ± 0.04 copies per diploid cell for mice that received low-dose and high-dose RV, respectively, as shown in Fig. 3A. We detected no RV sequences in two nontransduced MPS I mice. RV DNA sequences were undetectable at 2 months after transduction in two mice that received RV as adults and lost expression over time and were low at 0.007 copies/cell in mouse 8460, who maintained low levels of IDUA activity in serum.

doi:10.1016/j.ymthe.2004.08.027

Liver IDUA Activity

Liver homogenates from untreated MPS I mice had very low IDUA activity, as shown in Fig. 3B. This low level of activity may be due to the presence of other enzymes that can cleave the substrate 4-methylumbelliferyl α-L-iduronide with a low efficiency or may be due to low level contamination of the substrate with a compound that can be cleaved by other enzymes involved in degradation of GAGs. For mice that received low-dose RV as newborns and maintained serum IDUA activity at 28 U/ml, the liver IDUA activity was 5.9 ± 1.0 U/mg. For mice that received high-dose RV as newborns and maintained serum IDUA activity at 1029 U/ml, the liver IDUA activity was 289 ± 134 U/mg. Thus, IDUA activity in serum is directly proportional to that in liver. Both groups had higher liver IDUA activity than homozygous normal mice (4.2 ± 1 U/mg). Mice that received low-dose RV as newborns and lost expression over time had low liver IDUA activity (0.26 ± 0.14 U/mg), although this was higher than in MPS I mice. Two mice that received RV as adults had no liver IDUA activity, while the animal with some serum activity (8460) had 0.36 U/mg. In summary, mice that lost serum IDUA activity over time had low enzyme activity in the liver, which is consistent with the hypothesis that a cytotoxic T lymphocyte (CTL) response destroyed most of the transduced cells.

M6P Modification of IDUA in Serum

The hypothesis underlying this gene therapy approach is that liver will secrete M6P-modified IDUA into blood, and cells throughout the body will take enzyme up via the M6P receptor. Although 75.1 ± 3.3% of serum IDUA activity contained M6P for normal mice, this was only 8.0 ± 3.1 and 5.8 ± 0.4% ($P < 0.05$ vs. normal) for the low-dose and high-dose RV mice, respectively (Fig. 3C). Nevertheless, the average serum levels of M6P-modified IDUA for mice that received low-dose and high-dose RV and had 110 and 1240 U/ml total IDUA in serum were 8.8 and 72 M6P-modified U/ml, respectively. These values were higher than in normal mice (1.7 U/ml).

Clinical Evaluation

Mice received echocardiography, radiographs, bone mineral density (BMD) test, auditory-evoked brain-stem response (ABR) test, and electroretinogram (ERG) at 8 months after birth to evaluate cardiac, bone, ear, and eye disease. For the RV-treated mice, we evaluated only animals that received neonatal gene transfer and maintained expression at stable levels in serum. For all tests except radiographs and BMD, we evaluated only some of the mice from each group (as detailed in the figure legends) due to the cost and time involved. We chose animals whose average serum activity was approximately 30 and 1000 U/ml for the mice that received low-dose and high-dose RV, respectively.

Heart and Aorta

Cardiovascular disease resulting from lysosomal storage in arteries and heart valves is a major cause of death in patients with MPS I. All of 3 untreated MPS I mice had marked aortic dilatation (Fig. 4B) and showed evidence of aortic insufficiency (AI; Fig. 4F). None of 9 normal mice and none of 10 high-dose RV mice had aortic dilatation or AI ($P < 0.004$ with Fisher's exact test vs. MPS I). In contrast, 6 of 7 low-dose RV mice had aortic diameters greater than normal (Fig. 4C; $P < 0.001$), and 5 of 7 had AI (Fig. 4G; $P = 0.005$ vs. normal). Ascending aortas from MPS I and low-dose RV mice were dilated at the aortic valve annulus at 2.7 ± 0.2 and 2.4 ± 0.1 mm in diameter, respectively (Fig. 4I), and were even larger at the sinotubular junction at 3.1 ± 0.4 and 2.7 ± 0.2 mm, respectively (Fig. 4J). These were significantly greater ($P < 0.01$) than in normals, in which the diameter at the aortic valve annulus and the sinotubular junction was 1.9 ± 0.2 and 1.8 ± 0.2 mm, respectively. Values in high-dose RV mice were similar to those in normal mice. Echocardiographic parameters of left ventricular structure showed no significant changes in wall thickness, left ventricular mass index, or end-diastolic left ventricular chamber size, although values in the MPS I and low-dose RV mice tended to be greater, and the small sample sizes may limit our ability to detect differences. The fractional shortening (FS) was reduced in MPS I and low-dose RV mice at 43.3 ± 2.6 and 42 ± 6%, respectively (Fig. 4K). The FS in normal and high-dose RV mice was significantly greater at 52.6 ± 0.7 and 53.5 ± 1%, respectively ($P < 0.05$ for each group vs. MPS I). Low-dose RV mice had a significantly lower ($P < 0.05$) velocity of circumferential shortening at 11 ± 0.6 $ms^{-0.5}$ than did normal (13.3 ± 0.2) or high-dose RV (13.2 ± 0.4) mice (not shown). Mitral regurgitation was not detected in any mice (not shown).

We homogenized hearts and aortas and performed biochemical analyses. MPS I mice had very low IDUA activity in both organs. Low-dose RV mice had IDUA activity that was 0.3 ± 0.1 U/mg (13% of homozygous normal mice) in heart (Fig. 4L) and 0.5 ± 0.2 U/mg (14% of normal) in aorta (Fig. 4O). High-dose RV mice had IDUA activity that was >9-fold normal for both organs. Since MPS results in secondary elevation of other lysosomal enzymes and effective treatment normalizes these values, we measured the level of total β-hexosaminidase (β-hex) activity. MPS I mice had β-hex activity that was 12- and 10-fold that of normal for heart (Fig. 4M) and aorta (Fig. 4P), respectively ($P < 0.01$). Similarly, GAG levels were 17-fold normal at 6.8 ± 2.7 μg GAG/mg protein in heart (Fig. 4N; $P < 0.05$) and 83-fold normal at 174 μg GAG/mg protein in aorta (Fig. 4Q; $P < 0.01$). For low-dose RV mice, β-hex activity and GAG levels in the heart were slightly, albeit not statistically significantly, higher than in normal mice and were statistically lower than in MPS I mice. Aortic β-hex activity in low-dose RV mice was 7-fold normal, although this was not statistically different from values

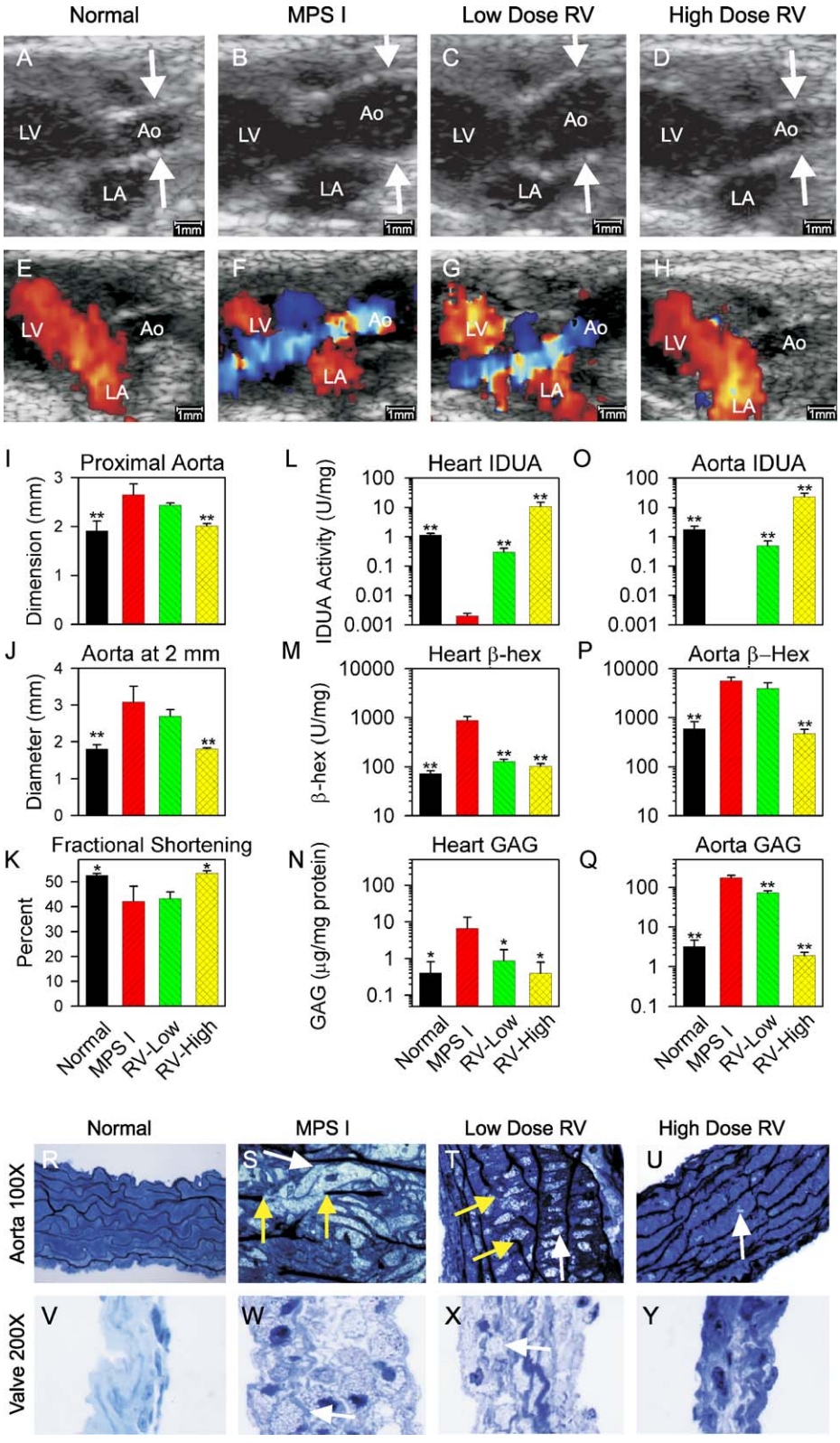

FIG. 4. Heart and aorta after neonatal gene therapy. Mice were untreated or treated with RV as newborns as described for Figs. 2A and 2B, and analyses were performed at 8 months on animals with stable expression. (A–D) 2-D echo of the aorta. End-diastolic parasternal long-axis images are shown, with the lumen of the aorta (Ao) and the cavity of the left ventricle (LV) and left atrium (LA) indicated. The white arrows indicate the wall of the aorta. The bar in each image represents 1 mm. (E–H) Color-Doppler of blood flow during diastole. In these middiastolic parasternal long-axis images, the blue indicates blood flow from the aorta to the left ventricle, which is diagnostic of AI. The red indicates normal blood flow from the left atrium to the left ventricle. (I–K) Quantitation of echocardiography. The average diameter ± SEM at the aortic valve annulus, the diameter at the aortic sinotubular junction, and the fractional shortening are shown for normal ($N = 9$), untreated MPS I ($N = 3$), low-dose RV ($N = 7$), and high-dose RV ($N = 10$) mice. Values in different groups in these and subsequent panels were compared using one-way ANOVA with Tukey post hoc analysis. $^{*}P = 0.01$ to 0.05 and $^{**}P < 0.01$ for comparison between MPS I mice and the other groups. (L–Q) IDUA activity, β-hex activity, and GAG levels in heart and aorta. Heart and aorta were homogenized ($N = 6$ for each group) and the IDUA activity, β-hex activity, and GAG levels were determined. (R–Y) Pathology in aorta and heart valve. Thin sections of the aorta (R–U; 100× original magnification) and mitral valve (V–Y; 200× original magnification) were stained with toluidine blue. The white arrows identify lysosomal storage material, which appears white. The yellow arrows in S and T identify regions where the elastic lamina appears fragmented.

doi:10.1016/j.ymthe.2004.08.027

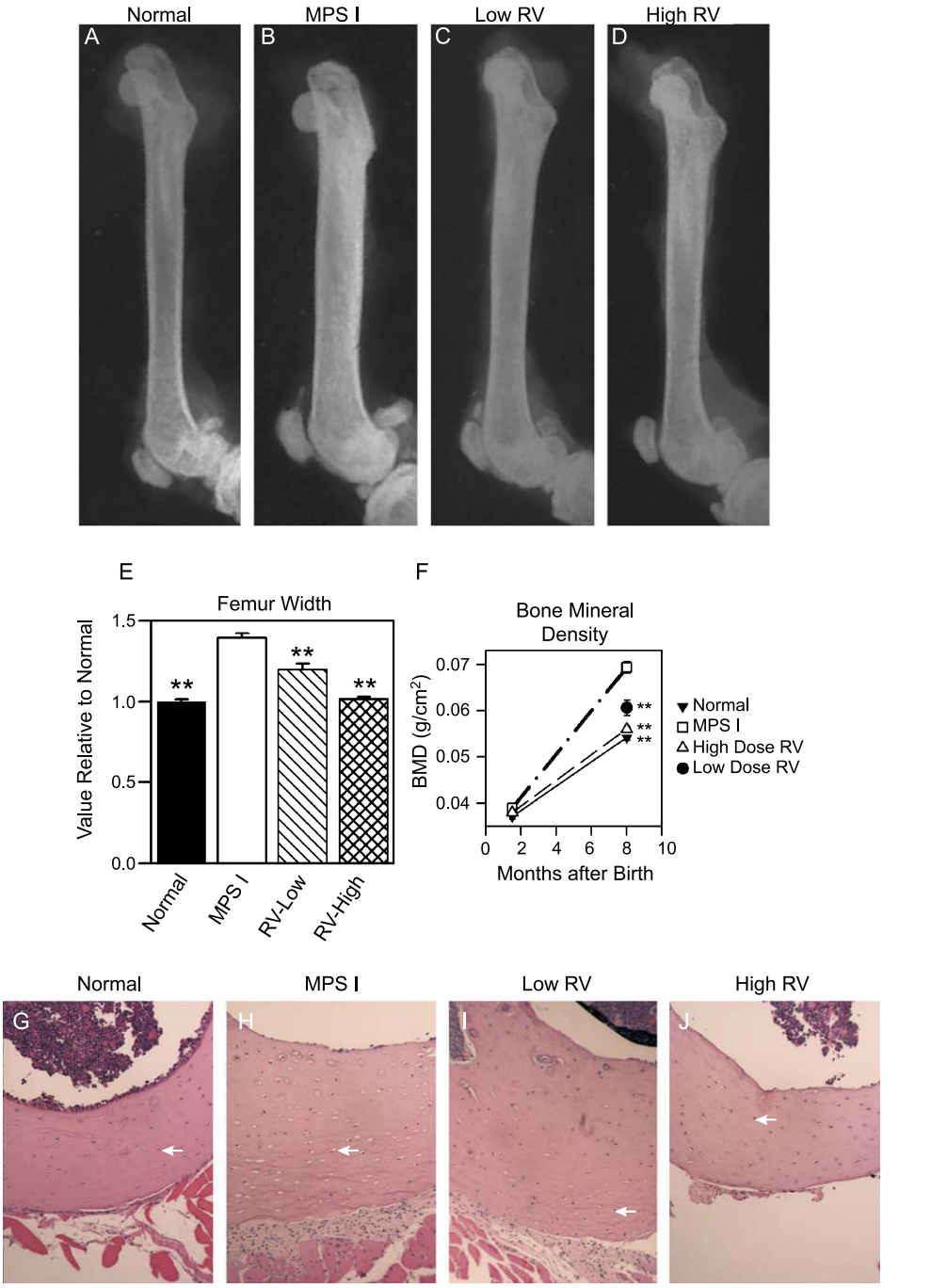

FIG. 5. Bones after neonatal gene therapy. Mice were untreated or treated with RV as newborns as described for Figs. 2A and 2B, and analyses were performed at 8 months unless otherwise stated. (A–D) Radiographs of the femur. (E) Femur diameter was measured from radiographs of normal ($N = 13$), untreated MPS I ($N = 11$), low-dose RV ($N = 12$), and high-dose RV ($N = 22$) mice, and the average values relative to that in normal mice ± SEM were determined. Statistical comparisons were between MPS I mice and the other groups as described for Fig. 4I. (F) Bone mineral density was determined at 6 weeks for normal ($N = 4$), untreated MPS I ($N = 6$), and high-dose RV ($N = 4$) mice and at 8 months for normal ($N = 11$), untreated MPS I ($N = 14$), low-dose RV ($N = 10$), and high-dose RV ($N = 15$) mice. (G–J) Pathology of bone. The cortical bone was stained with hematoxylin and eosin (20× original magnification). The inner surface of the cortex is at the top and white arrows indicate osteocytes in the cortical bone.

in MPS I or normal mice. Aortic GAG levels in low-dose RV mice were 22-fold normal at 73.5 μg GAG/mg protein ($P < 0.05$), although this was only 42% of the value in MPS I mice ($P < 0.01$). β-Hex and GAG levels were normal in both organs in the high-dose RV mice.

We also assessed the degree of correction of lysosomal storage by histopathology. MPS I mice had ++++ storage in the aorta (Fig. 4S) and mitral valve (Fig. 4W). Storage was absent from most regions (+) for high-dose RV mice (Figs. 4U and 4Y), but was only modestly reduced (+++) for low-dose RV mice (Figs. 4T and 4X). Since there were many regions where the elastic lamina was discontinuous for MPS I and low-dose RV mice, loss of structural integrity may result in the aortic dilatation observed in these groups. The storage that was present (++++) in the interstitial cells of the myocardium of MPS I mice was absent (0) in high-dose and low-dose RV mice (data not shown). We conclude that high-dose RV prevented echocardiographic, biochemical, and pathological manifestations of cardiac disease. Low-dose RV reduced storage in the myocardium, but had only a modest effect in the aorta and heart valves. The inability of 14% of normal IDUA activity in the aorta in low-dose RV mice to prevent disease may be due to unequal distribution of enzyme throughout the aorta.

Bone Radiographs and BMD

Skeletal disease results in cosmetic and functional abnormalities in patients with MPS I. A femur from an MPS I mouse was wider at 1.4 ± 0.03-fold normal ($P < 0.01$) and was more sclerotic on a radiograph obtained at 8 months (Figs. 5B and 5E) than for a normal mouse. The width abnormality was completely corrected in the high-dose RV mice ($P < 0.01$ vs. MPS I) and was partially corrected to 1.2 ± 0.1-fold normal for low-dose RV mice ($P < 0.01$ vs. MPS I). However, the diameter remained higher in low-dose RV than in normal mice ($P < 0.01$).

To quantify sclerosis, we tested BMD, as shown in Fig. 5F. For MPS I mice, the BMD was indistinguishable from that in normals at 6 weeks, but was markedly elevated at 0.069 ± 0.004 g/cm^2 at 8 months ($P < 0.01$ vs. normal). The BMD was 0.056 ± 0.002 g/cm^2 in the high-dose RV group at 8 months, which was not different from the value of 0.054 ± 0.002 in normal mice, but was lower than in MPS I mice ($P < 0.01$ vs. MPS I). The BMD was 0.060 ± 0.005 in the low-dose RV group, which was lower than in MPS I mice ($P < 0.01$) but higher than in normals ($P < 0.01$). Pathological evaluation of cross sections demonstrated that femurs of MPS I mice have osteocytes with ++++ lysosomal storage and a thick cortex (Fig. 5H). Osteocyte storage and bone thickness were completely corrected in high-dose RV mice (Fig. 5J). Low-dose RV mice (Fig. 5I) had storage in some osteocytes (+) and a thick cortex. We conclude that high-dose and low-dose RV result in marked and partial improvements in bones, respectively.

Auditory Function

Since MPS I results in reduced hearing, we performed ABR. As shown in Fig. 6, MPS I mice had markedly reduced hearing at 8 months at frequencies of 5 and 10 kHz, with auditory thresholds of 84 ± 1 and 76 ± 7 dB, respectively. There were no statistically significant differences between any of the groups at 20 and 40 kHz, which is likely due to the high-frequency hearing deficit in C57BL/6 mice [25]. The hearing threshold in mice that received low-dose RV at 10 kHz was 39.4 ± 5.2 dB, which was not statistically different from values in normal mice, but was lower than in MPS I mice ($P < 0.01$). However, at 5 kHz the hearing threshold of 59.4 ± 4.5 dB was not statistically improved from that in MPS I mice. The hearing in the high-dose RV group was indistinguishable from that in normal mice. We conclude that high-dose and low-dose RV result in complete and partial improvement in hearing, respectively.

Visual Function

MPS I can reduce retinal function and cause corneal clouding. The initial hyperpolarization (a-wave) in response to light of a dark-adapted ERG (Fig. 7) reflects rod photoreceptor function, while the depolarization that follows (b-wave) indicates function of photoreceptors and secondary neurons [12]. The a- and b-wave amplitudes at −124 ± 19 (SEM) and 452 ± 58 μV, respectively, in MPS I mice at 8 months (Figs. 7A–7C) were markedly less than in normal mice, in which the values were −346 ± 11 ($P < 0.01$) and 735 ± 25 μV ($P < 0.01$), respectively. This indicates that MPS I mice have reduced rod photoreceptor function. Low-dose RV a-wave amplitudes were statistically different at −256 ± 29 mV from both normal ($P < 0.01$) and MPS I ($P < 0.01$) mice, showing partial improvement. The b-wave in low-dose RV mice was 646 ± 39 μV, which was statistically better than in MPS I mice ($P < 0.05$), but was not statistically different from normal mice. Values in mice that received high-dose RV were similar to normal and statistically better than in MPS I mice ($P < 0.01$).

Pathological evaluation of the eye demonstrated that MPS I mice had only 6.3 ± 0.3 cells/thickness in the outer nuclear layer of the photoreceptors (Figs. 7D and 7F), which was less than the value of 10.9 ± 0.3 cells/thickness in normal mice ($P < 0.01$). The low-dose RV mice had 8.2 ± 0.2 cells/thickness, which was higher than in MPS I mice ($P < 0.05$) but lower than in normals ($P < 0.01$). The number of cells/thickness in the high-dose RV mice was normal at 11.1 ± 0.4 cells/thickness. The outer segments of the photoreceptors were short and disordered in MPS I mice and long and regular in normal mice. The outer segments were normal and improved in high-dose and low-dose RV mice, respectively. These pathologic abnormalities in photoreceptor cells in MPS I mice likely contributed to the reduced retinal function detected on ERG, while

doi:10.1016/j.ymthe.2004.08.027

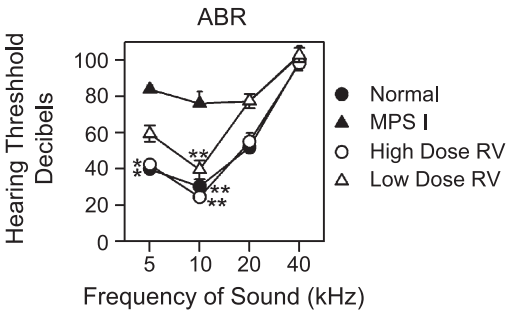

FIG. 6. Hearing after neonatal gene therapy. Mice were untreated or treated with RV as newborns as described for Figs. 2A and 2B, and hearing was evaluated by ABR at 8 months. The average hearing threshold ± SEM at the indicated frequencies of sound was determined for normal ($N = 11$), untreated MPS I ($N = 7$), low-dose RV ($N = 5$), and high-dose RV ($N = 10$) mice. Statistical comparisons were between MPS I mice and the other groups.

partial and complete correction of the pathology in low-dose and high-dose RV mice, respectively, correlates with the degree of correction in the ERG. MPS I mice also had substantial lysosomal storage (++++) in the cornea (Fig. 7J). Storage in the corneal stroma and endothelium was partially (varied from + to ++) and completely (0) corrected with low-dose (Fig. 7K) and high-dose (Fig. 7L) RV, respectively. We conclude that RV improves the ERG and eye pathology in a dose-dependent fashion.

DISCUSSION

The goal of this study was to determine if liver-targeted gene therapy could correct the clinical manifestations of MPS I in mice. Neonatal gene therapy with a high dose (10^9 TU/kg) of an RV expressing canine IDUA resulted in stable expression of IDUA in serum in all (25 of 25) animals for 8 months at 1240 ± 147 U/ml (564-fold levels in homozygous normals). Administration of low-dose RV (10^8 TU/kg) resulted in stable expression in most (13 of 17) animals at 110 ± 31 U/ml (50-fold normal), although 4 of 17 (24%) either lost expression over time or had low expression at the first time of analysis. Since the latter mice had very low liver IDUA activity (Fig. 3B) and did not produce anti-cIDUA antibodies (data not shown), a CTL response that destroyed the transduced cells may have occurred. Thus, although neonatal administration of an RV expressing other proteins induced tolerance in mice and dogs [26], it may be necessary to modulate the immune response at the time of gene therapy to newborns with MPS I to achieve stable expression consistently.

The amount of M6P-modified IDUA secreted into blood can be estimated based upon the serum IDUA activity and the percentage of enzyme with M6P if one assumes that the half-life of the mannose 6-phosphorylated canine enzyme in mice is 19 min, which is the half-life of human IDUA in dogs [27]. Thus, animals that received high-dose RV secreted (1000 U/ml) × (50% produced during a half-life) × (5.8% mannose 6-phosphorylated/total enzyme in serum) × (35 ml of serum/kg body weight), which is 1015 units of M6P-modified IDUA/kg every 19 min, or 539,000 units with M6P/kg/week. The secretion for low-dose RV mice with 30 U/ml total serum IDUA activity can similarly be calculated at 22,000 units with M6P/kg/week. For comparison, we consider that humans [28] or cats [29] that received 125,000 U/kg/week of IDUA received high-dose ERT, while cats [29] and dogs [30] that received 25,000 U/kg/week received low-dose ERT. It should be noted, however, that enzyme activity with our assay at 37°C was approximately fourfold higher than when the same samples were assayed under the conditions used to monitor IDUA activity for these ERT studies (data not shown), which were room temperature with a lower concentration of substrate. Additional caveats are that there may be species-related differences in the half-life of the IDUA and the percentage of enzyme with M6P was not stated in the half-life study.

The percentage of serum IDUA with M6P was much lower in RV-transduced MPS I (7%) than in normal (75%) mice. For human IDUA, the N-linked oligosaccharides that contain M6P are attached at N336 and N451 [31]. Although both these sites are conserved in murine IDUA [32], there is an alanine at the position homologous to N451 for the canine protein [20]. This might result in a lower efficiency of M6P modification of the canine than of the murine protein, a hypothesis that is currently being tested. Enzyme might also be taken up by cells of the reticuloendothelial system via the mannose receptor, as the human IDUA protein has oligosaccharides with high mannose at N372 and N415 [20], and these sites are conserved in the canine protein.

Cardiac Disease

Valvular and arterial disease of the heart are a major cause of death in patients with MPS I. In this study, 8-month-old untreated MPS I mice had an aortic valve annulus diameter that was 138% of normal, which would result in an area 191% of normal. This aortic dilatation is likely the major cause of AI, although we cannot rule out a contribution from an abnormal aortic valve. Furthermore, MPS I mice had an FS that was 80% of normal. These results are consistent with reports that MPS I mice can have dilated hearts [16] and abnormal echocardiograms [33].

In this study, echocardiograms in MPS I mice that received high-dose RV at birth were completely normal. Although functional evaluation of the effects of different treatments on cardiac disease has not previously been evaluated in mice with MPS, these results are consistent with the substantial correction of cardiac disease in MPS VII dogs that received neonatal gene therapy with an RV

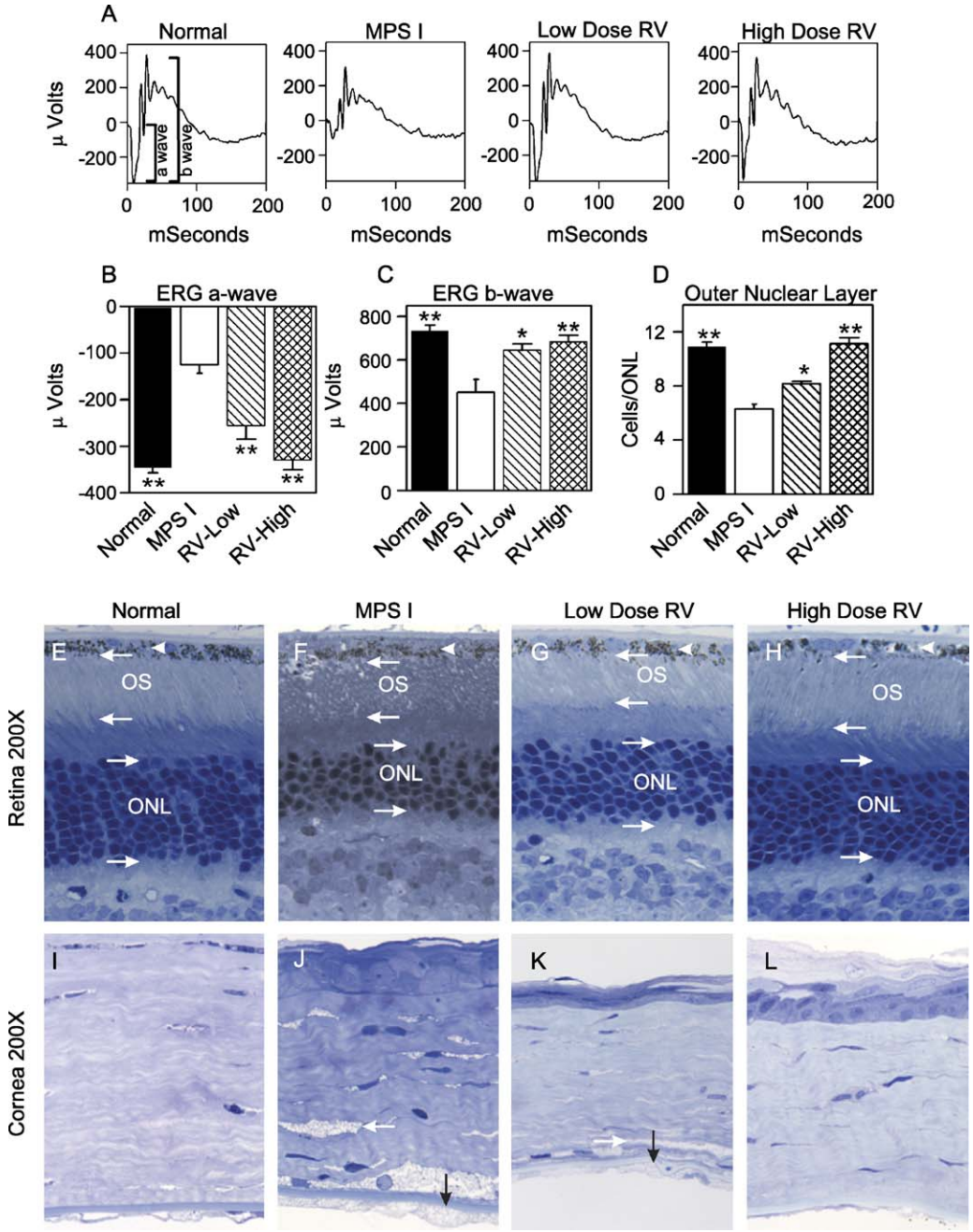

FIG. 7. Vision after neonatal gene therapy. Mice were untreated or treated with RV as newborns as described for Figs. 2A and 2B, and eyes were evaluated at 8 months. (A) Representative flash ERGs from dark-adapted mice are shown. (B) a-wave amplitude. The average magnitude of the a-wave ± SEM was determined from the dark-adapted ERG of normal (N = 12), untreated MPS I (N = 7), low-dose RV (N = 7), and high-dose RV (N = 11) mice. Statistical comparisons were between MPS I mice and the other groups as described for Fig. 4I. (C) b-wave amplitude. The average magnitude of the dark-adapted b-wave was determined from the same animals shown in B. (D) Outer nuclear layer thickness. The number of cells from anterior to posterior in the outer nuclear layer was determined for normal (N = 5), MPS I (N = 5), low-dose RV (N = 3), and high-dose RV (N = 4) mice and the average ± SEM determined. (E–H) Pathology in the retina. The posterior of the retina is at the top. White arrows that point to the left identify the edges of the outer segments (OS) of the photoreceptors, white arrows that point to the right identify the edges of the outer nuclear layer (ONL) of the photoreceptors, and the white arrowhead identifies the retinal pigmented epithelium. Original magnification 200×. (I–L) Pathology in the cornea. The white and black arrows identify corneal fibroblasts and corneal endothelial cells with lysosomal storage material, respectively.

doi:10.1016/j.ymthe.2004.08.027

expressing GUSB [14]. Complete correction of cardiac manifestations has not been achieved with ERT or BMT, although these were initiated at a later age. For example, although BMT at ~2 years improved clinical symptoms in most patients, AI developed or worsened in all patients after 10 years [34]. Similarly, dogs that received BMT still had mitral valve and arterial medial thickening, although these were reduced, and aortic root dilatation was absent [35,36]. Initiation of high-dose ERT in humans at ~12 years did not normalize echocardiograms in most patients at 1 year, and mitral regurgitation worsened in some [28]. The failure of low-dose ERT to improve pathological and/or echocardiographic manifestations of disease in cats [29] and dogs [30] is consistent with our finding that low-dose RV (which should deliver less enzyme with M6P to blood as did low-dose ERT) did not prevent cardiac disease.

Bone

Dysostosis multiplex results in a broad and short face, with adverse cosmetic consequences, and thickened abnormally formed bones that reduce mobility. In this study, MPS I mice had femur diameters and BMD that were 40 and 28% greater, respectively, than values in normal mice. The elevated BMD in MPS I mice in our study has not been noted previously and differs from the reduction in BMD reported in MPS I dogs [30], although decreased mobility in the dogs may have reduced the BMD. Femur diameter and BMD abnormalities, as well as the short and broad face (data not shown), were completely and partially corrected with high-dose and low-dose RV, respectively. This is consistent with the marked improvements in craniofacial aspects of bone disease noted with neonatal AAV vector-mediated gene therapy [24]. Bone disease has not been corrected with BMT or ERT in other species with MPS I. For example, no or little improvement was noted in humans that received BMT at ~2 years [37] or initiated ERT at ~12 years [28] or in dogs that received low-dose ERT [30]. It is likely that the early age of treatment in this and the neonatal AAV vector study in mice [24] was critical for achieving this degree of improvement in bone.

Although bones were sclerotic and thickened in MPS I mice as previously reported [16], long bone lengths in MPS I male mice were not significantly different from normal and in females were normal for the tibia and humerus and only modestly reduced in the femur at 95.0 $\pm$ 1% of normal ($P < 0.05$ vs. normal) (data not shown). This differs from results in untreated MPS VII mice, in which the long bones were <86% of normal [7,10]. This difference is likely due to the fact that the growth plate is much less abnormal in MPS I than in MPS VII mice (data not shown), which is probably related to accumulation of chondroitin sulfate in MPS VII but not MPS I. Since bone lengths have not been completely corrected in MPS VII with any therapy [7,10], this difference suggests that it may be easier to correct bone disease in MPS I than in MPS VII.

Hearing

In MPS VII mice, hearing deficits are caused by conductive defects, which may be due in part to bone sclerosis, and sensorineural abnormalities [25]. In this study, MPS I mice had markedly reduced hearing on ABR at 8 months. Mice that received high-dose RV at birth had normal hearing, which may be due in part to reduced sclerosis of bones. Those that received low-dose RV had improved hearing, although substantial deficits remained. Hearing has improved or stabilized after BMT in human patients [38]. Hearing was only partly corrected after neonatal AAV vector-mediated gene therapy in mice with MPS VII [11], which might relate to the larger size of GUSB than IDUA or the need for higher levels of GUSB than IDUA.

Vision

Patients with MPS I have reduced vision due to abnormalities in retinal function and corneal clouding. In this study, MPS I mice had reduced rod function, as dark-adapted responses to a flash of light were abnormal (Fig. 7). The cone function was relatively intact, as the light-adapted b-wave at 8 months was normal (data not shown). Similarly, rods were more severely affected than cones on ERG in humans with MPS I [39]. In this study, treatment with high-dose and low-dose RV resulted in complete and partial correction of dark-adapted ERG, respectively. Improvements in ERG were likely due to improved function of photoreceptors, whose outer nuclear layer and outer segments were abnormal in MPS I mice, but appeared normal or improved in those that received high-dose or low-dose RV, respectively. Humans with MPS I that received BMT at 1 to 7 years of age had initial improvements in ERG, but these were not sustained 5 years later [40]. ERG was only partly corrected after BMT [12] or localized AAV-mediated gene therapy [13] in MPS VII mice.

Corneal clouding also contributes to decreased visual acuity. In this study, MPS I mice had substantial lysosomal storage in the cornea, which causes corneal clouding. High-dose and low-dose RV resulted in complete and partial correction, respectively, of lysosomal storage in the cornea. In other studies, most patients with MPS I that received BMT still had some corneal clouding, although improvements were noted [38,40]. Corneal clouding did not improve in humans that received ERT for 1 year starting at ~12 years after birth, although one patient had improved visual acuity [28]. Corneal clouding was reduced, but not eliminated, with BMT [36,41] or low-dose ERT [30] in dogs and was reduced in one cat that received high-dose ERT, but not in another high-dose ERT cat or in low-dose ERT cats [29]. In MPS VII mice, lysosomal storage in the cornea was corrected with BMT

and neonatal RV-mediated gene therapy, but not with ERT [5,10].

Implications for Patients with MPS I

We demonstrate here that MPS I mice that received neonatal gene therapy with a high dose of an RV expressing cIDUA achieved 58 U/ml M6P-modified IDUA in serum and had marked improvements in cardiac, bone, ear, and eye disease. These improvements are more complete than reported for humans or large animals that received BMT or ERT, although the early age of treatment in this study was almost certainly important. However, gene therapy in large animals may be less efficacious than in small animals, and humans may be more mature at birth, making them less amenable to a neonatal approach. BM-directed gene therapy to adults reduced lysosomal storage in liver, spleen, and brain in MPS I mice, although other organs were not evaluated [23], while neonatal AAV vector-mediated gene therapy improved bone disease [24]. It is clear that high secretion is important for an optimal clinical effect, as mice that received low-dose RV and achieved 2.4 U/ml M6P-modified IDUA in serum had partial or no improvements. These data help to define a target level of IDUA activity in serum, which will need to be confirmed in large animals prior to using this approach in humans. Although important, the only part of the central nervous system evaluated here was the retina. Studies to evaluate the pathology in the brain are in progress.

Although the magnitude of the clinical effect in mice with neonatal gene therapy is profound, most patients with MPS I are not diagnosed at birth [42] and this neonatal approach will only be useful if newborn screening is implemented [43]. It will therefore be critical to evaluate the clinical effect of gene therapy in older animals. This was not possible here, as mice that received gene therapy as adults had a dramatic fall in the serum IDUA activity at 2 to 3 weeks after transduction. This decline was probably due to a CTL response, as the liver had low RV DNA copies (Fig. 3A) and IDUA activity (Fig. 3B), and antibodies were not detected (data not shown). Immune responses have also occurred in other species. Antibodies developed in humans [28], cats [29], and dogs [30] after ERT and in dogs after muscle-directed [44] or nonmyeloablative BM-directed [45] gene therapy. Although antibodies were prevented in dogs with immunosuppressive agents [46], it is unclear if this regimen would block a CTL response. Further studies will attempt to achieve stable levels of IDUA in blood in adult mice using transient immunosuppression and determine the clinical effect.

This approach should be used in humans only if long-term analysis demonstrates that adverse effects of neonatal gene therapy with an RV are rare. Induction of tumors in liver or other organs due to insertional mutagenesis is of particular concern due to the leukemias that recently developed in patients that received RV-mediated gene therapy for severe combined immunodeficiency [47]. In this study, animals that received high-dose RV had 0.17 ± 0.04 copies per diploid cell at 8 months after transduction. This should represent ~10^6 total transduction events if one assumes that each transduced cell generated 35 hepatocytes during growth of newborns into adults, the liver is 4% of the body weight, and there are 1.7×10^8 hepatocytes per gram of liver [48]. Although no liver tumors have developed to date in mice or dogs that received neonatal gene therapy with an RV, longer analysis is necessary. If the risk of an adverse event is sufficiently low, this neonatal gene therapy approach would be a simple and effective way to prevent most somatic manifestations of MPS I.

Materials and Methods

All reagents were purchased from Sigma Chemical (St. Louis, MO, USA) unless otherwise stated. Statistical analyses were performed with SigmaStat (Sigma Chemical).

Generation of hAAT-cIDUA-WPRE and in vitro transduction. An *Eco*RI fragment containing the 2.2-kb canine IDUA cDNA [20] was blunt-end ligated into the *Not*I site of hAAT-WPRE-767 [8]. An amphotropic RV was purified and shown to lack replication-competent retrovirus as detailed previously [8]. To determine the titer, murine 3521 cells [5] were transduced overnight with RV. One week later, cells were harvested and the DNA copy number and IDUA activity determined.

Animals. MPS I knockout mice generated by insertion into exon 6 of the 14-exon *IDUA* gene [17] in a C57BL/6 background were generously supplied by Dr. Elizabeth Neufeld. Some homozygous MPS I mice received 100 μl of RV via the temporal vein at 2–3 days after birth. Other homozygous MPS I and heterozygous normal littermates did not receive any treatment at birth. Some homozygous adult (6-week-old) MPS I mice were injected with a cumulative dose of human HGF [49] of 25 mg/kg over 12 h and RV was injected via the tail vein at 30, 36, and 48 h after the first dose of HGF, as described previously [50]. Serum was obtained from blood from the orbital plexus of the right eye. At 8 months, some mice received echocardiography with an Acuson Sequoia Echocardiography System C256 (Siemens Medical Solutions Ultrasound Division, Mountain View, CA, USA) with a 15L8 high-frequency transducer under light anesthesia with 2,2,2-tribromoethanol (2.5% solution, 5 μl/g body wt). BMD was performed with a PixiMus dual energy X-ray absorption machine (Lunar, Madison WI, USA), ABR was performed as described [25], and flash ERG was performed on the left eye after dark-adaptation for at least 3 h as described [12,13]; these were performed under anesthesia with 80 mg/kg ketamine and 15 mg/kg xylazine given intraperitoneally. Prior to sacrifice, blood was collected, and the animals were transcardially perfused with 20 ml of saline.

IDUA activity, β-hexosaminidase activity, and GAG levels. Cells or organs were homogenized in lysis buffer as described [23] and the same homogenate was used for enzyme and GAG assays. The total protein concentration was determined with the Bradford assay (Bio-Rad Laboratories, Hercules, CA, USA). IDUA and total β-hex assays were performed using 4-methylumbelliferyl-α-L-iduronide (Calbiochem, San Diego, CA, USA) and 4-methylumbelliferyl-2-acetamido-2deoxy-β-glucopyranoside, respectively, as substrates as described [23] except that the IDUA assay was performed for 1 to 6 h at 37°C with an equal volume of 100 μM substrate. The fluorescence in a blank that got the same amount of substrate as the samples and was incubated for the same period of time was subtracted prior to calculation of activity. One unit of enzyme releases 1 nmol of 4-methylumbelliferone per hour. IDUA activity in organs from homozygous

doi:10.1016/j.ymthe.2004.08.027

normal mice was assumed to be twice the level determined for heterozygous normal mice. GAGs were determined using a sulfated glycosaminoglycan kit from Blyscan (Newtownabbey, Northern Ireland) with chondroitin 4-sulfate as the standard. To evaluate the M6P content of IDUA in serum, samples from five mice were pooled to give ~1 ml. This was loaded onto a M6P receptor column, and the fraction of enzyme activity that bound and was eluted with M6P was determined as described [6].

Anti-cIDUA antibody assay. Purified canine IDUA was generously provided by Emil Kakkis. ELISA plates were coated with 5 μg/ml cIDUA in PBS, serum samples were diluted at 1:100 or higher, and IgG antibodies were detected with a horseradish peroxidase-coupled anti-mouse IgG antibody as described [50]. Samples were negative if the OD was less than twice the background obtained using a well that was coated with PBS only.

DNA copy number. Cells or organs were homogenized in guanidinium and extracted DNA was used for real-time PCR with Taqman technology (Applied Biosystems, Rockville, MD, USA). Primers specific for the WPRE of the RV and for mouse β-actin were used to determine the DNA copy number [5]. Standards were DNA from mouse cells that contained 1 copy of hAAT-cGUSB-WPRE per cell that were diluted with DNA from nontransduced mouse liver.

Pathological evaluation. Pieces of organs were fixed and embedded in plastic, and 1-μm sections were stained with toluidine blue as previously described [5,13]. Bone was fixed for 1 day with formalin and decalcified for 4 days with 14% EDTA, and 5-μm sections were stained with hematoxylin and eosin. Pathology was evaluated without knowledge of the genotype or treatment status and was scored as normal (0), storage in some but not all regions (+), or small (++), moderate (+++), or severe (++++) amounts of storage in all regions.

ACKNOWLEDGMENTS

We thank Elizabeth Neufeld for the canine IDUA cDNA and the MPS I mice, Clay Semenkovich and Trey Coleman for assistance with BMD, Mark Sands for helpful discussions, and Emil Kakkis for purified canine IDUA. This work was supported by the Ryan Foundation, the National MPS Society, and the National Institutes of Health (DK66448 awarded to K.P.P. and RO3 DC04946 awarded to A.K.H.). Histology was supported by P30 DK52574, EY02687, DC04665, and Research to Prevent Blindness. BMD equipment was supported by the Clinical Nutrition Research Unit (DK56341) and the Diabetes Research Training Core (DK20579). ERG and ABR equipment were supported by the James S. McDonnell Foundation. Echocardiography equipment was supported by the Mouse Cardiovascular Phenotyping Core Facility at the Center for Cardiovascular Research.

RECEIVED FOR PUBLICATION JULY 16, 2004; ACCEPTED AUGUST 31, 2004.

REFERENCES

1. Meikle, P. J., Hopwood, J. J., Clague, A. E., and Carey, W. F. (1999). Prevalence of lysosomal storage disorders. *JAMA* **281:** 249–254.
2. Desnick, R. J. (2004). Enzyme replacement and enhancement therapies for lysosomal diseases. *J. Inherit. Metab. Dis.* **27:** 385–410.
3. Cheng, S. H., and Smith, A. E. (2003). Gene therapy progress and prospects: gene therapy of lysosomal storage disorders. *Gene Ther.* **10:** 1275–1281.
4. Neufeld, E. F., and Muenzer, J. (2001). The mucopolysaccharidoses. In *Metabolic and Molecular Basis of Inherited Disease* (B. A. Scriver, W. S. Sly, D. Valle Eds.), pp. 3421–3452. McGraw–Hill, New York.
5. Xu, L., Mango, R. L., Sands, M. S., Haskins, M. E., Ellinwood, N. M., and Ponder, K. P. (2002). Evaluation of pathological manifestations of disease in mucopolysaccharidosis VII mice after neonatal hepatic gene therapy. *Mol. Ther.* **6:** 745–758.
6. Ponder, K. P., *et al.* (2002). Therapeutic neonatal hepatic gene therapy in mucopolysaccharidosis VII dogs. *Proc. Natl. Acad. Sci. USA* **99:** 13102–13107.
7. Mango, R. L., *et al.* (2004). Neonatal retroviral vector-mediated hepatic gene therapy reduces bone, joint, and cartilage disease in mucopolysaccharidosis VII mice and dogs. *Mol. Genet. Metab.* **82:** 4–19.
8. Xu, L., *et al.* (2002). Transduction of hepatocytes after neonatal delivery of a Moloney murine leukemia virus-based retroviral vector results in long-term expression of β-glucuronidase in mucopolysaccharidosis VII dogs. *Mol. Ther.* **5:** 141–153.
9. Xu, L., *et al.* (2004). In vivo transduction of hematopoietic stem cells after neonatal intravenous injection of an amphotropic retroviral vector in mice. *Mol. Ther.* **10:** 37–44.
10. Vogler, C., Barker, J., Sands, M. S., Levy, B., Galvin, N., and Sly, W. S. (2001). Murine mucopolysaccharidosis VII: impact of therapies on the phenotype, clinical course, and pathology in a model of a lysosomal storage disease. *Pediatr. Dev. Pathol.* **4:** 421–433.
11. Daly, T. M., Ohlemiller, K. K., Roberts, M. S., Vogler, C. A., and Sands, M. S. (2001). Prevention of systemic clinical disease in MPS VII mice following AAV-mediated neonatal gene transfer. *Gene Ther.* **8:** 1291–1298.
12. Ohlemiller, K. K., Vogler, C. A., Roberts, M., Galvin, N., and Sands, M. S. (2000). Retinal function is improved in a murine model of a lysosomal storage disease following bone marrow transplantation. *Exp. Eye Res.* **71:** 469–481.
13. Hennig, A. K., Ogilvie, J. M., Ohlemiller, K. K., Timmers, A. M., Hauswirth, W. W., and Sands, M. S. (2004). AAV-mediated intravitreal gene therapy reduces lysosomal storage in the retinal pigmented epithelium and improves retinal function in adult MPS VII mice. *Mol. Ther.* **10:** 106–116.
14. Sleeper, M. M., *et al.* (2004). Gene therapy ameliorates cardiovascular disease in dogs with mucopolysaccharidosis VII. *Circulation* **110:** 815–820.
15. Lowry, R. B., Applegarth, D. A., Toone, J. R., MacDonald, E., and Thunem, N. Y. (1990). An update on the frequency of mucopolysaccharide syndromes in British Columbia. *Hum. Genet.* **85:** 389–390.
16. Clarke, L. A., *et al.* (1997). Murine mucopolysaccharidosis type I: targeted disruption of the murine alpha-L-iduronidase gene. *Hum. Mol. Genet.* **6:** 503–511.
17. Ohmi, K., Greenberg, D. S., Rajavel, K. S., Ryazantsev, S., Li, H. H., and Neufeld, E. F. (2003). Activated microglia in cortex of mouse models of mucopolysaccharidoses I and IIIB. *Proc. Natl. Acad. Sci. USA* **100:** 1902–1907.
18. Haskins, M. E., Jezyk, P. F., Desnick, R. J., McDonough, S. K., and Patterson, D. F. (1979). Alpha-L-iduronidase deficiency in a cat: a model of mucopolysaccharidosis I. *Pediatr. Res.* **13:** 1294–1297.
19. Shull, R. M., Munger, R. J., Spellacy, E., Hall, C. W., Constantopoulos, G., and Neufeld, E. F. (1982). Canine alpha-L-iduronidase deficiency: a model of mucopolysaccharidosis I. *Am. J. Pathol.* **109:** 244–248.
20. Stoltzfus, L. J., *et al.* (1992). Cloning and characterization of cDNA encoding canine alpha-L-iduronidase: mRNA deficiency in mucopolysaccharidosis I dog. *J. Biol. Chem.* **267:** 6570–6575.
21. Ashton, L. J., Brooks, D. A., McCourt, P. A., Muller, V. J., Clements, P. R., and Hopwood, J. J. (1992). Immunoquantification and enzyme kinetics of alpha-L-iduronidase in cultured fibroblasts from normal controls and mucopolysaccharidosis type I patients. *Am. J. Hum. Genet.* **50:** 787–794.
22. Bunge, S., Clements, P. R., Byers, S., Kleijer, W. J., Brooks, D. A., and Hopwood, J. J. (1998). Genotype–phenotype correlations in mucopolysaccharidosis type I using enzyme kinetics, immunoquantification and in vitro turnover studies. *Biochim. Biophys. Acta* **1407:** 249–256.
23. Zheng, Y., Rozengurt, N., Ryazantsev, S., Kohn, D. B., Satake, N., and Neufeld, E. F. (2003). Treatment of the mouse model of mucopolysaccharidosis I with retrovirally transduced bone marrow. *Mol. Genet. Metab.* **79:** 233–244.
24. Hartung, S. D., *et al.* (2004). Correction of metabolic, craniofacial, and neurologic abnormalities in MPS I mice treated at birth with adeno-associated virus vector transducing the human alpha-L-iduronidase gene. *Mol. Ther.* **9:** 866–875.
25. Ohlemiller, K. K., Hennig, A. K., Lett, J. M., Heidbreder, A. F., and Sands, M. S. (2002). Inner ear pathology in the mucopolysaccharidosis VII mouse. *Hear. Res.* **169:** 69–84.
26. Zhang, J., Xu, L., Haskins, M. E., and Ponder, K. P. (2004). Neonatal gene transfer with a retroviral vector results in tolerance to human factor IX in mice and dogs. *Blood* **103:** 143–151.
27. Shull, R. M., Kakkis, E. D., McEntee, M. F., Kania, S. A., Jonas, A. J., and Neufeld, E. F. (1994). Enzyme replacement in a canine model of Hurler syndrome. *Proc. Natl. Acad. Sci. USA* **91:** 12937–12941.
28. Kakkis, E. D., *et al.* (2001). Enzyme-replacement therapy in mucopolysaccharidosis I. *N. Engl. J. Med.* **344:** 182–188.
29. Kakkis, E. D., *et al.* (2001). Enzyme replacement therapy in feline mucopolysaccharidosis I. *Mol. Genet. Metab.* **72:** 199–208.
30. Kakkis, E. D., *et al.* (1996). Long-term and high-dose trials of enzyme replacement therapy in the canine model of mucopolysaccharidosis I. *Biochem. Mol. Med.* **58:** 156–167.
31. Zhao, K. W., Faull, K. F., Kakkis, E. D., and Neufeld, E. F. (1997). Carbohydrate structures of recombinant human alpha-L-iduronidase secreted by Chinese hamster ovary cells. *J. Biol. Chem.* **272:** 22758–22765.
32. Clarke, L. A., *et al.* (1994). Murine alpha-L-iduronidase: cDNA isolation and expression. *Genomics* **24:** 311–316.
33. Zheng, Y., Jordan, M. C., Rozengurt, N., Roos, K. P., and Neufeld, E. F. (2003). Cardiac malfunction in the mouse model of Hurler syndrome (MPS I). *FASEB J.* **17:** A528.
34. Braunlin, E. A., *et al.* (2003). Usefulness of bone marrow transplantation in the Hurler syndrome. *Am. J. Cardiol.* **92:** 882–886.
35. Gompf, R. E., Shull, R. M., Breider, M. A., Scott, J. A., and Constantopoulos, G. C. (1990). Cardiovascular changes after bone marrow transplantation in dogs with mucopolysaccharidosis I. *Am. J. Vet. Res.* **51:** 2054–2060.
36. Breider, M. A., Shull, R. M., and Constantopoulos, G. (1989). Long-term effects of bone marrow transplantation in dogs with mucopolysaccharidosis I. *Am. J. Pathol.* **134:** 677–692.

37. Field, R. E., Buchanan, J. A., Copplemans, M. G., and Aichroth, P. M. (1994). Bone-marrow transplantation in Hurler's syndrome: effect on skeletal development. *J. Bone Joint Surg. Br.* **76:** 975–981.

38. Guffon, N., Souillet, G., Maire, I., Straczek, J., and Guibaud, P. (1998). Follow-up of nine patients with Hurler syndrome after bone marrow transplantation. *J. Pediatr.* **133:** 119–125.

39. Caruso, R. C., Kaiser-Kupfer, M. I., Muenzer, J., Ludwig, I. H., Zasloff, M. A., and Mercer, P. A. (1986). Electroretinographic findings in the mucopolysaccharidoses. *Ophthalmology* **93:** 1612–1616.

40. Gullingsrud, E. O., Krivit, W., and Summers, C. G. (1998). Ocular abnormalities in the mucopolysaccharidoses after bone marrow transplantation: longer follow-up. *Ophthalmology* **105:** 1099–1105.

41. Constantopoulos, G., Scott, J. A., and Shull, R. M. (1989). Corneal opacity in canine MPS I: changes after bone marrow transplantation. *Invest. Ophthalmol. Visual Sci.* **30:** 1802–1807.

42. Cleary, M. A., and Wraith, J. E. (1995). The presenting features of mucopolysaccharidosis type IH (Hurler syndrome). *Acta Paediatr.* **84:** 337–339.

43. Meikle, P. J., and Hopwood, J. J. (2003). Lysosomal storage disorders: emerging therapeutic options require early diagnosis. *Eur. J. Pediatr.* **162:** S34–37.

44. Shull, R. M., Lu, X., McEntee, M. F., Bright, R. M., Pepper, K. A., and Kohn, D. B. (1996). Myoblast gene therapy in canine mucopolysaccharidosis. I. Abrogation by an immune response to alpha-L-iduronidase. *Hum. Gene Ther.* **7:** 1595–1603.

45. Lutzko, C., *et al.* (1999). Genetically corrected autologous stem cells engraft, but host immune responses limit their utility in canine alpha-L-iduronidase deficiency. *Blood* **93:** 1895–1905.

46. Kakkis, E., *et al.* (2004). Successful induction of immune tolerance to enzyme replacement therapy in canine mucopolysaccharidosis I. *Proc. Natl. Acad. Sci. USA* **101:** 829–834.

47. Hacein-Bey-Abina, S., *et al.* (2003). LMO2-associated clonal T cell proliferation in two patients after gene therapy for SCID-X1. *Science* **302:** 415–419.

48. Gates, G. A., Henley, K. S., Pollard, H. M., Schmidt, E., and Schmidt, F. W. (1961). The cell populations of the human liver. *J. Lab. Clin. Med.* **57:** 182–184.

49. Gao, C., *et al.* (1999). Lipopolysaccharide potentiates the effect of hepatocyte growth factor on hepatocyte replication in rats by augmenting AP-1 activity. *Hepatology* **30:** 1405–1416.

50. Xu, L., *et al.* (2003). Neonatal or hepatocyte growth factor-potentiated adult gene therapy with a retroviral vector results in therapeutic levels of canine factor IX for hemophilia B. *Blood* **101:** 3924–3932.